[3] S. Gao, P. Gardner, and S. T. Chiw, "Broadband integrated antenna for LINC systems," *Microw. Opt. Technol. Lett.*, vol. 33, no. 2, pp. 93–95, Apr. 2002.
[4] S. Gao and P. Gardner, "Novel integrated antenna for LINC power amplifiers," in *Proc. IEEE Int. Antennas Propag. Symp.*, Jun. 2002, vol. 2, pp. 508–511.
[5] S. Gao and P. Gardner, "Integrated antenna/power combiner for LINC radio transmitters," *IEEE Trans. Microw. Theory Techn.*, vol. 53, no. 3, pp. 1083–1088, Mar. 2005.
[6] C. Liang and B. Razavi, "Transmitter linearization by beam forming," *IEEE J. Solid-State Circuits*, vol. 46, no. 9, pp. 1956–1969, Sep. 2011.
[7] M. A. Elaal and F. Ghannouchi, "A modified LINC amplification system for wireless transceivers," in *Proc. IEEE 46th Veh. Technol. Conf. (VTC-06 Fall.)*, 2006, pp. 1–3, doi: 10.1109/VTCF.2006.600.
[8] F. Benahmed Daho *et al.*, "An operational modified-LINC demonstrator for wireless communication," in *Proc. 5th Eur. Conf. Antennas Propag. (EUCAP'11)*, Apr. 2011, pp. 480–482.
[9] A. Birafane, M. El-Asmar, A. B. Kouki, M. Helaoui, and F. M. Ghannouchi, "Analyzing LINC systems," *IEEE Microw. Mag.*, vol. 11, no. 5, pp. 59–71, Aug. 2010.
[10] Y. Zhou, M. Y.-W. Chia, X. Qing, and J. Yuan, "RF spatial modulation using antenna arrays," *IEEE Trans. Antennas Propag.*, vol. 61, no. 10, pp. 5229–5236. Oct. 2013.
[11] W. Shen, C Xue, K. K. Mei, and J. Lin, "Maxwellian circuits of conducting circular loops," *IEEE Trans. Antennas Propag.*, vol. 59, no. 10, pp. 3848–3854, Oct. 2011.
[12] G. Zhou and G. S. Smith, "An accurate theoretical model for the thinwire circular half-loop antenna," *IEEE Trans. Antennas Propag.*, vol. 39, no. 8, pp. 1167–1177, Aug. 1991.
[13] U. Johannsen, "Technologies for integrated millimeterwave antennas," Ph.D. dissertation, Eindhoven Univ. Technology, Eindhoven, The Netherlands, 2013 [Online]. Available: http://alexandria.tue.nl/extra2/754833.pdf.
[14] A. Voors, *4nec2 Antenna Modeling and Optimizing Software, Version 5.8.11*, May 2005 [Online]. Available: http://www.qsl.net/4nec2/
[15] G. J. Burke and A. J. Poggio, "Numerical electromagnetics code (NEC)—Method of moments," Naval Ocean Systems Center, San Diego, CA, USA, NOSC Tech. Document 116, Jan. 1981.
[16] CST Microwave Studio, Darmstadt, Germany, 2009 [Online]. Available: http://www.cst.com

Compact Broadband Dual-Polarized Antenna for Indoor MIMO Wireless Communication Systems

Hyunwoo Lee and Byungje Lee

***Abstract*—A compact $(100\ \text{mm} \times 100\ \text{mm} \times 40\ \text{mm})$ dual-polarized antenna with wide impedance bandwidth and high isolation is proposed for an indoor MIMO wireless communication system. The proposed antenna consists of cavity-backed bowtie antennas with parasitic elements. It can cover the DCS/PCS/UMTS/LTE 1, 2, 3, 4, 7, 9, 10, 15, 16, 23, 25 bands (1710–2690 MHz). The wide impedance bandwidth $(\text{VSWR} < 2)$, of about 44.5%, is achieved by using parasitic elements with optimal location and length and the cavity of an electrical wall. High-isolation $(>31\ \text{dB})$ and low-envelop correlation coefficient $(\text{ECC} < 0.00425)$ between MIMO elements are achieved by orthogonal dual-polarization while suppressing the cross-polarization of each MIMO antenna element. The peak gain is higher than 7 dBi in the entire operating frequency band.**

***Index Terms*—Cavity-backed antenna, high isolation, MIMO antenna, parasitic elements, polarization diversity.**

I. Introduction

Miniature indoor base stations or repeaters for mobile wireless communications systems have been installed in shaded areas, such as inside of buildings, underground construction areas, and in tunnels to provide steadier wireless communication services regardless of place [1]–[4]. In line with the need to provide improved performance for mobile wireless communication systems, the demand for high-channel capacity and wider coverage has rapidly increased. Long term evolution (LTE) is one of the key technologies in recent mobile wireless communication services. LTE can provide improved system capacity and coverage, reliable high peak data rate, and enhanced spectrum efficiency. One of the key technologies for LTE services is the multiple-input multiple-output (MIMO) system that can enhance data reliability, channel capacity, and network coverage in multipath environments using multiple antennas without additional power. For indoor base stations or repeaters covering various mobile wireless communications systems, such as DCS/PCS/UMTS/LTE bands, the most important recent issue is how to design compact multiband MIMO antennas with a low cost and how to obtain good isolation between closely spaced MIMO antenna elements where antennas must be designed within a small volume.

Various techniques have been studied for achieving high isolation in the design of the MIMO antenna [5]–[13]. The simplest method to achieve high isolation is to use the spatial diversity technique that requires a physically separated distance of more than 0.5 λ between MIMO antenna elements. This technique may not be suitable for small indoor base stations or repeaters of mobile wireless communications systems where MIMO antennas must be designed within a small volume [5]. The defected ground structure (DGS), which operates as a band-stop filter due to the combination of inductance and capacitance,

Manuscript received April 26, 2015; revised August 17, 2015; accepted November 25, 2015. Date of publication December 07, 2015; date of current version February 01, 2016. This work was supported by a Research Grant from Kwangwoon University in 2015.

The authors are with the Department of Wireless Communications Engineering, Kwangwoon University, Seoul 139-701, Korea (e-mail: bj_lee@kw.ac.kr).

Color versions of one or more of the figures in this communication are available online at http://ieeexplore.ieee.org.

Digital Object Identifier 10.1109/TAP.2015.2506201

is able to achieve high isolation [6]. It is however difficult to implement the modification of the ground plane of the MIMO antenna in widespread commercial procedures. The polarization diversity is one of the alternative techniques used to realize high isolation within a compact volume. The polarization purity, which refers to the ratio of copolarization to cross-polarization, decreases rapidly when one antenna is operated in the higher order mode [7], [8]. To obtain low cross-polarization and high isolation, additional techniques must be applied with the polarization diversity in the design of the broadband MIMO antenna. The shorting pin between the MIMO antenna elements and the ground plane is applied to improve isolation by minimizing the mutual coupling between MIMO antenna elements due to the shared PCB ground plane [9]. The decoupling network has also been used to obtain high isolation [10], [11]. The structure of the antenna, including the decoupling network, becomes more complicated. A MIMO antenna with different types of antenna elements, such as a patch antenna and a slot antenna, can result in high isolation. It is however difficult to optimize a MIMO antenna's performance due to the unbalanced ratio of antenna gain between the MIMO antenna elements [12], [13].

In this communication, a compact $(100\ \text{mm} \times 100\ \text{mm} \times 40\ \text{mm})$ broadband dual-polarized MIMO antenna is proposed for miniature indoor base stations or repeaters of recent mobile wireless communications systems. Two linearly polarized bowtie antennas are used as MIMO antenna elements (MIMO antenna 1 and MIMO antenna 2) and are orthogonally positioned to obtain high isolation between them once closely mounted. Using the cavity-backed bowtie antenna in conjunction with additional parasitic elements, wider impedance bandwidth and high isolation are achieved. The impedance bandwidth $(\text{VSWR} < 2)$ of the proposed MIMO antenna can cover the existing 3G service bands (DCS/PCS/UMTS) and LTE bands (LTE 1, 2, 3, 4, 7, 9, 10, 15, 16, 23, 25) (1710–2690 MHz). High isolation $(>31\ dB)$ and low ECC (<0.00425) between the proposed MIMO antenna elements are achieved by realizing an orthogonal polarization between them and by suppressing the cross-polarization that may lead to unwanted mutual coupling. The measured peak gain is higher than 7 dBi.

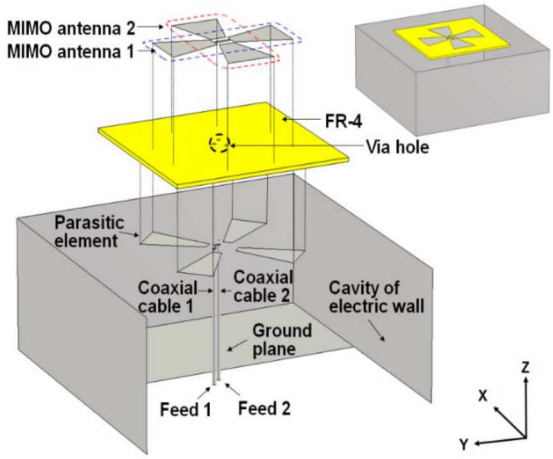

(a)

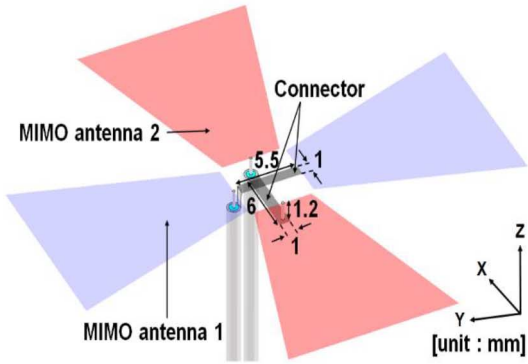

(b)

Fig. 1. Structure of the proposed MIMO antenna. (a) Overall view. (b) Detailed view of MIMO antenna elements and coaxial feeds.

II. Antenna Configuration and Design Concept

Fig. 1(a) shows the overall structure of the proposed cavity-backed MIMO antenna. It consists of two radiating elements (MIMO antenna 1 and MIMO antenna 2) mounted on the FR-4 substrate ($\varepsilon_r = 4.3$ and thickness $= 1.2$ mm), parasitic elements, a square cavity, and two coaxial feeds. The radiating elements are bowtie antennas, which are mounted on the FR-4 substrate orthogonally to each other. The four parasitic elements, which are arranged along diagonal lines ($\phi = \pm 45^\circ$), are located on the bottom of the FR-4 substrate. The radiating elements are excited by two coaxial feeds. Fig. 1(b) shows a detailed view of the proposed MIMO antenna structure presenting the connection between the MIMO antenna elements and coaxial cables. For each MIMO antenna element, the inner conductor of a coaxial cable is connected to one arm of a bowtie antenna, and the outer conductor of a coaxial cable is connected to the other arm of a bowtie antenna by the connector. The overall size, including the cavity, is 100 mm $\times$ 100 mm $\times$ 40 mm.

Fig. 2 shows the detailed geometry and dimensions of the proposed MIMO antenna. Fig. 3 presents structures of four different types of MIMO antennas. Type I is composed of radiating elements (MIMO antenna 1 and MIMO antenna 2), the ground plane, and coaxial feeds. Type II is designed by applying four additional parasitic elements to Type I. Type III is a cavity-backed form of Type I. Type IV (proposed MIMO antenna) is a cavity-backed form of Type II, which is achieved by simultaneously adding both the parasitic elements and the cavity to Type I without additional volume expansion.

Fig. 4 presents simulated reflection coefficients (dB magnitude of S_{11}) and isolations (dB magnitude of S_{21}) for Types I, II, III, and IV (proposed MIMO antenna). It is observed that S_{22} and S_{12} are similar to S_{11} and S_{21}, respectively. Fig. 4(a) shows that Types II and III give a wider impedance bandwidth than that of Type I. The wider impedance bandwidth of Type II is accomplished by dual resonance. The first and second resonances occurred due to the bowtie elements and by parasitic elements, respectively. The length of the parasitic elements is $\lambda_e/4$, where λ_e is the effective wavelength at 2.5 GHz, improving the impedance bandwidth. With the optimal location and length, the parasitic element can act as an impedance matching element, and can then provide a wider impedance bandwidth. The cavity-backed antenna helps Type III achieve a wider impedance bandwidth [14], [15]. This shows that the impedance bandwidth $(\text{VSWR} < 2)$ of Types II and III is still insufficient and unable to cover the entire operating frequency band (1710–2690 MHz). Fig. 4(a) shows that the proposed MIMO antenna (Type IV), which has both the parasitic elements and the square cavity, gives a sufficient broad bandwidth to cover the entire operating frequency band. Fig. 4(b) shows that the isolation of Type

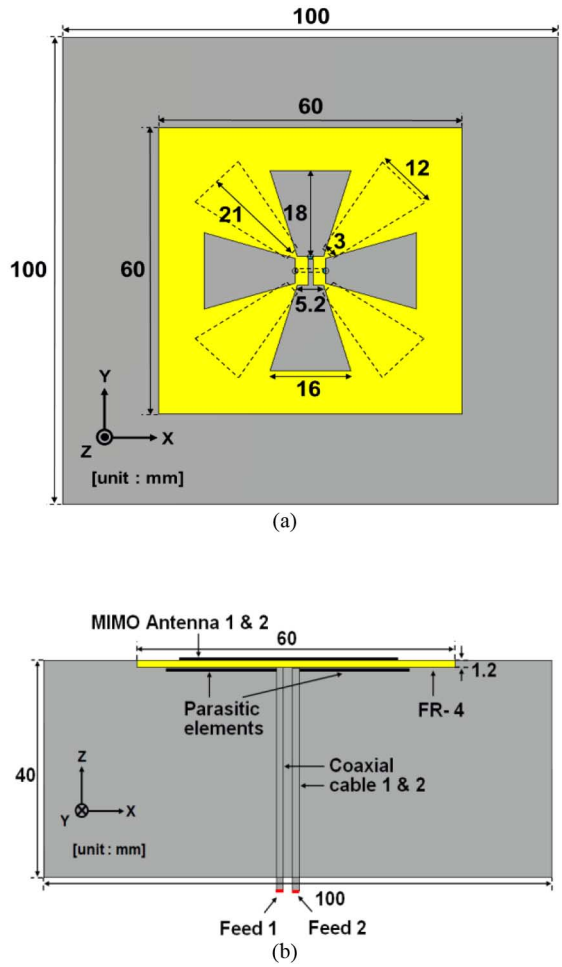

Fig. 2. Detailed geometry and dimension of the proposed MIMO antenna. (a) Front view. (b) Side view.

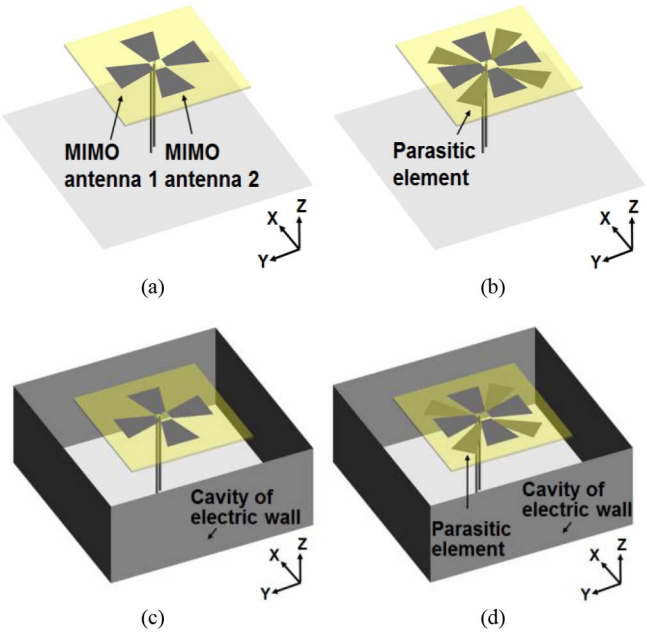

Fig. 3. Structures of different types of MIMO antennas. (a) Type I. (b) Type II. (c) Type III. (d) Type IV (proposed MIMO antenna).

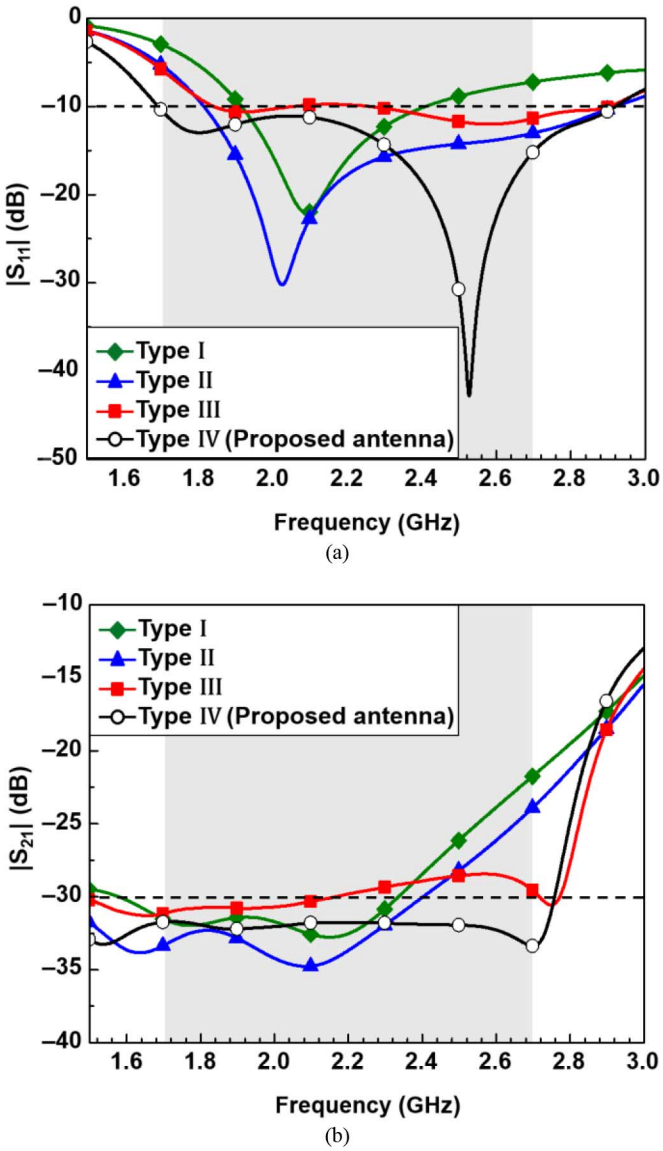

Fig. 4. Simulated S-parameters for different antenna types. (a) S_{11}. (b) S_{21}.

II is slightly improved compared to that of Type I due to the parasitic elements. Fig. 5 shows the current distribution on Types I and II. When MIMO antenna 1 is excited and MIMO antenna 2 is terminated to a load with 50 Ω, the eddy current is induced on MIMO antenna 2 for both Types I and II. The current is also induced on the four parasitic elements of Type II. It is observed that the currents on the parasitic elements and the MIMO antenna 2 produce fields that cancel somewhat in the far field, since most currents are opposite-directed. Isolation between MIMO antenna 1 and MIMO antenna 2 of Type II can be therefore higher than that of Type I by reducing mutual coupling between MIMO antenna elements in conjunction with the diagonal arrangement of the parasitic elements. Fig. 4(b) shows that Type III results in a higher isolation than that of Types I and II in high-frequency band only. It is also observed that the proposed MIMO antenna (Type IV) only allows a higher isolation ($>$30 dB) for the entire operating frequency band in cooperation with the cavity and parasitic elements.

Fig. 6 shows the simulated copolarization and cross-polarization radiation patterns of MIMO antenna 1 for Types II and IV (proposed

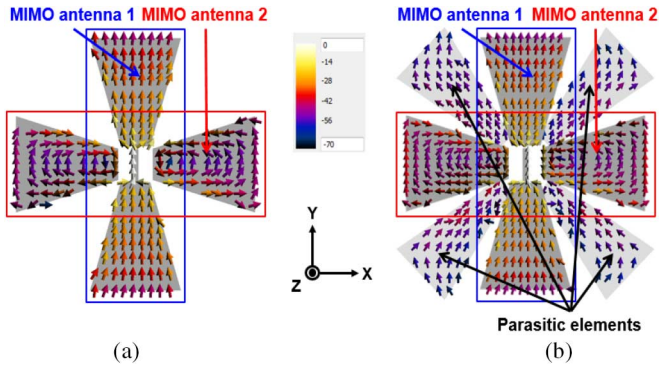

Fig. 5. Current distribution at 2.4 GHz. (a) Type I. (b) Type II.

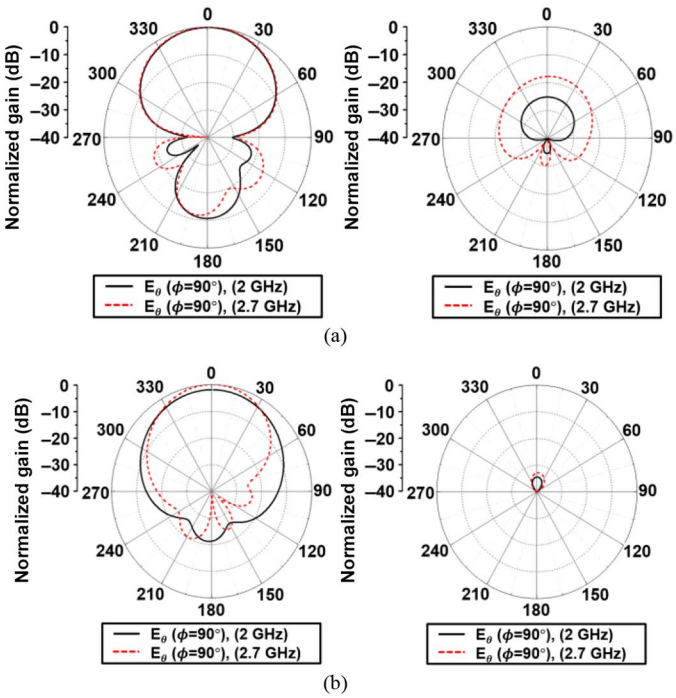

Fig. 6. Simulated radiation patterns of copolarization and cross-polarization of MIMO antenna 1 at 2 GHz and at 2.7 GHz (yz-plane). (a) Type II. (b) Type IV (proposed MIMO antenna).

MIMO antenna). Simulated results are obtained by using SPEAG's SEMCAD X [16]. Fig. 6(a) shows that while the copolarization patterns of Type II at 2 GHz and at 2.7 GHz are almost identical, the cross-polarization is greater at 2.7 GHz than at 2 GHz. Fig. 6(b) shows that the proposed MIMO antenna has a cross-polarization of less than –33 dB at both 2 and 2.7 GHz. It is observed that the cavity-backed bowtie antenna with parasitic elements can minimize the cross-polarization, so that the proposed MIMO antenna delivers better polarization purity and higher isolation ($>$30 dB). A slight difference in copolarization patterns at 2 and 2.7 GHz for Type IV is due to the extension of the ground plane using the cavity of the electric wall. Fig. 6(b) shows that the gain at 2.7 GHz is slightly higher than that at 2 GHz since the electrical dimension of the cavity at 2.7 GHz is larger than that at 2 GHz. Type II has a small size of the ground plane without a cavity compared to Type IV; Fig. 6(a) shows almost identical copolarization patterns at 2 and 2.7 GHz.

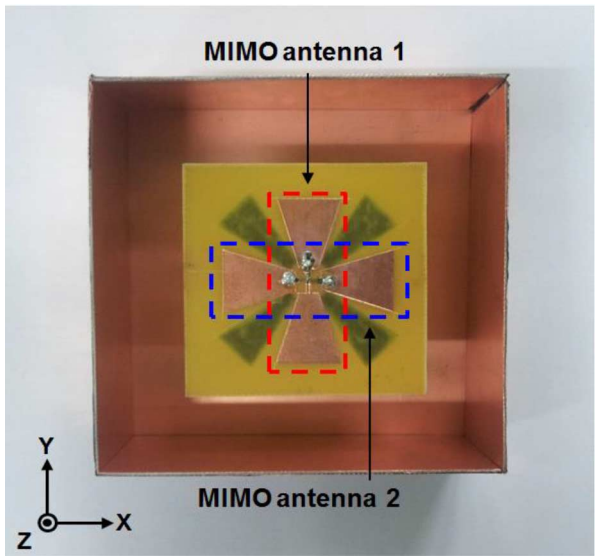

Fig. 7. Photograph of the fabricated proposed antenna.

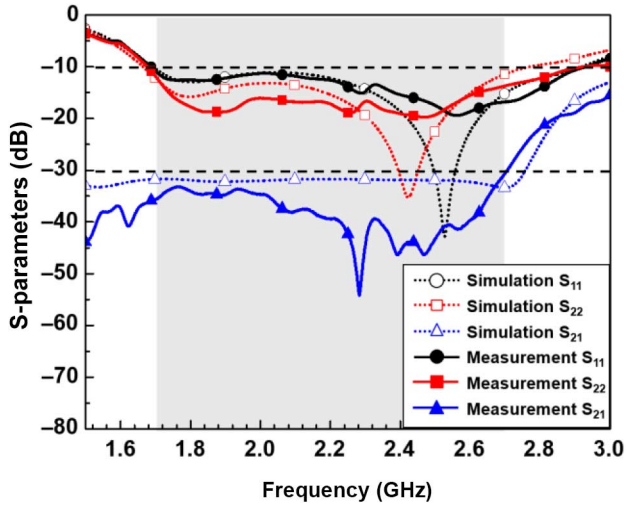

Fig. 8. S-parameters of the proposed MIMO antenna.

III. Measured Results

Fig. 7 shows a photograph of the fabricated proposed MIMO antenna. Fig. 8 shows the simulated and measured S-parameters of the proposed MIMO antenna. It is observed that the proposed MIMO antenna has a sufficiently wide impedance bandwidth (VSWR $<$ 2) to cover the entire operating frequency band (1710–2690 MHz) and that the measured isolation (S_{21}) between MIMO antennas elements is higher than 31 dB. Fig. 9 shows the simulated and measured ECC by using the far-field radiation patterns [17]. The proposed MIMO antenna has a low ECC ($<$0.00425), which means that MIMO antennas 1 and 2 operate independently improving capacity [18]. Fig. 10 shows the measured copolarization and cross-polarization radiation patterns of MIMO antenna 1. The proposed MIMO antenna has a much lower cross-polarization. It is observed that the measured radiation patterns of MIMO antenna 2 are similar to those of MIMO antenna 1, but their polarizations are orthogonal to each other. Fig. 11 presents the simulated and measured peak gains of the proposed MIMO antenna, showing that the measured peak gains of both MIMO antennas 1 and 2 are greater than 7 dBi in all operating frequency bands. The measured and simulated results agree well. Radiation patterns and peak gains

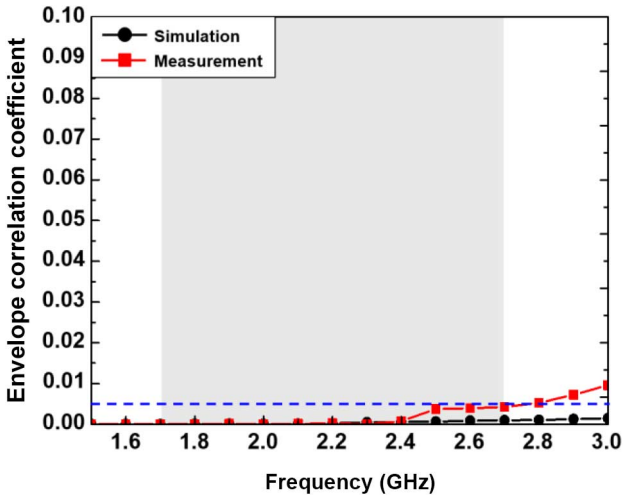

Fig. 9. Simulated and measured envelope correlation coefficient (ECC).

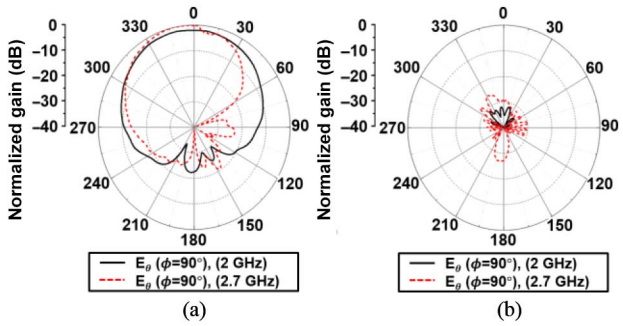

Fig. 10. Measured radiation patterns of proposed MIMO antenna 1 at 2 and 2.7 GHz (yz-plane). (a) Copolarization. (b) Cross-polarization.

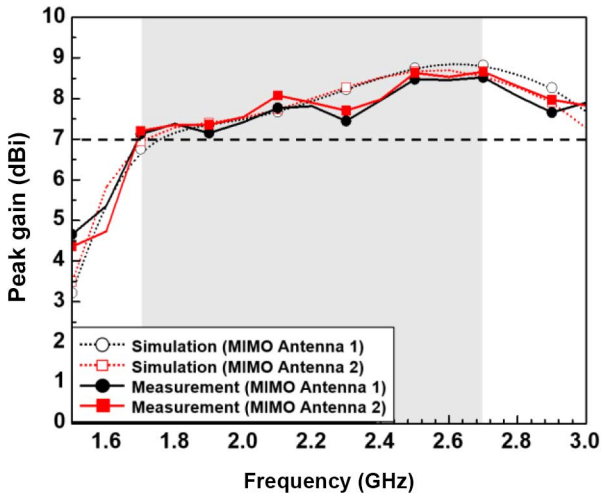

Fig. 11. Peak gain of the proposed antenna.

were measured with one antenna excited and the other terminated to a load with 50 Ω.

IV. Conclusion

A compact broadband dual-polarized cavity-backed bowtie MIMO antenna is proposed to achieve wide impedance bandwidth, high isolation, and low cross-polarization. Using both the parasitic elements and the square cavity, the proposed antenna provides sufficient broad bandwidth (VSWR < 2) to cover the entire operating frequency band (1710–2690 MHz: DCS/PCS/UMTS bands and LTE 1, 2, 3, 4, 7, 9, 10, 15, 16, 23, 25 bands). The proposed antenna radiates orthogonal dual-polarized waves to enhance the isolation between MIMO antenna elements. The cavity-backed bowtie antenna with an optimal location and length of the parasitic elements is achieved with a higher isolation ($>$31 dB) and low ECC ($<$0.00425). High-peak gain ($>$7 dBi) is also achieved. The proposed MIMO antenna could be a good candidate for practical indoor base stations or repeaters for recent mobile wireless communications systems in the industry since it is compact (100 mm $\times$ 100 mm $\times$ 40 mm) and can reduce manufacturing cost.

References

[1] M. N. Patwary, P. B. Rapajic, and I. Oppermann, "Capacity and coverage increase with repeaters in UMTS urban cellular mobile communication environment," *IEEE Trans. Commun.*, vol. 53, no. 10, pp. 1620–1624, Oct. 2005.

[2] J. Borkowski, J. Niemela, T. Isotalo, P. Lahdekorpi, and J. Lempiainen, "Utilization of an indoor DAS for repeater deployment in WCDMA," in *Proc. IEEE 63th Veh. Technol. Conf.*, Melbourne, VIC, Australia, 2006, pp. 1112–1116.

[3] K. Hiltunen, "Using RF repeaters to improve WCDMA HSDPA coverage and capacity inside buildings," in *Proc. IEEE 17th Int. Symp. Pers. Indoor Mobile Radio Commun.*, Helsinki, Finland, 2006, pp. 1–5.

[4] C. X. Wang, X. Hong, X. Ge, G. Zhang, and J. Thompson, "Cooperative MIMO channel models: A survey," *IEEE Commun. Mag.*, vol. 48, no. 2, pp. 80–87, Feb. 2010.

[5] G. Chi, B. Li, and D. Qi, "A dual-frequency antenna fed by CPW," in *Proc. IEEE Antennas Propag. Soc. Int. Symp.*, Washington, DC, USA, 2005, pp. 459–462.

[6] D. Guha, M. Biswas, and Y. M. M. Antar, "Microstrip patch antenna with defected ground structure for cross polarization suppression," *IEEE Antennas Wireless Propag. Lett.*, vol. 4, no. 1, pp. 455–458, Dec. 2005.

[7] T. Huynh, K. F. Lee, and R. Q. Lee, "Cross-polarization characteristics of rectangular patch antennas," *Electron. Lett.*, vol. 24, pp. 463–464, Apr. 1988.

[8] Z. N. Chen and M. Y. W. Chia, "Experimental study on radiation performance of probe-fed suspended plate antennas," *IEEE Trans. Antennas Propag.*, vol. 51, no. 8, pp. 1964–1971, Aug. 2003.

[9] B. Li, Y. Z. Yin, W. Hu, Y. Ding, and Y. Zhao, "Wideband dual-polarized patch antenna with low cross polarization and high isolation," *IEEE Antennas Wireless Propag. Lett.*, vol. 11, pp. 427–430, Apr. 2012.

[10] J. J. Xie, Y. Z. Yin, J. H. Wang, and X. L. Liu, "Wideband dual-polarised electromagnetic fed patch antenna with high isolation and low cross-polarisation," *Electron. Lett.*, vol. 49, no. 3, pp. 171–173, Jan. 2013.

[11] T. W. Chiou and K. L. Wong, "Broad-band dual-polarized single microstrip patch antenna with high isolation and low cross polarization," *IEEE Trans. Antennas Propag.*, vol. 50, no. 3, pp. 399–401, Mar. 2002.

[12] K. L. Wong and T. W. Chiou, "Broadband dual-polarized patch antennas fed by capacitively coupled feed and slot-coupled feed," *IEEE Trans. Antennas Propag.*, vol. 50, no. 3, pp. 346–351, Mar. 2002.

[13] S. Y. Suh, V. K. Nair, D. Souza, and S. Gupta, "High isolation antenna for multi-radio antenna system using a complementary antenna pair," in *Proc.IEEE Antennas Propag. Soc. Int. Symp.*, Honolulu, HI, USA, 2007, pp. 1229–1232.

[14] K. Nichizawa, H. Ohashi, and Y. Konishi, "An orthogonal dual polarized all-metal cavity-backed patch antenna with low cross polarization," in *Proc. IEEE Antennas Propag. Soc. Int. Symp.*, San Diego, CA, USA, 2008, pp. 1–4.

[15] M. Mazanek, P. Pechac, and M. Polivka, "Cavity-backed patch antennas," in *10th Int. Conf. Antennas Propag.*, Edinburgh, U.K., pp. 126–129.

[16] *SEMCAD X*, SPEAG, Zurich, Switzerland, 2010 [Online]. Available: http://www.semcad.com

[17] S. Blanch, J. Romeu, and I. Corbella, "Exact representation of antenna system diversity performance from input parameter description," *Electron. Lett.*, vol. 39, no. 9, pp. 705–707, May 2003.

[18] J. Xiong, M. Zhao, H. Li, Z. Ying, and B. Wang, "Collocated electric and magnetic dipoles with extremely low correlation as a reference antenna for polarization diversity MIMO applications," *IEEE Antennas Wireless Propag. Lett.*, vol. 11, pp. 423–426, Apr. 2012.